Optimum Interplanetary Rendezvous With Power-Limited Vehicles

W. G. MELBOURNE[1] AND C. G. SAUER JR.[2]

Jet Propulsion Laboratory, California Institute of Technology, Pasadena, Calif.

The optimum thrust programs for power-limited propulsion systems are used to generate rendezvous trajectories from Earth to Mars for various flight times and launch dates during the years 1968 to 1971. The manner in which the propulsion requirements vary with flight time and launch date is considered, and a comparison of vehicle performance using the variable and constant thrust programs is presented. The existence of optimum launch dates is interpreted in terms of certain transversality conditions derivable from the calculus of variations. A brief comparison of the advanced propulsion vehicle and the ballistic vehicle propulsion requirements is made for Earth-Mars rendezvous trajectories.

THE emergence of advanced propulsion for interplanetary flights has generated great interest in the application of optimization theory to advanced propulsion vehicle systems and to trajectory design. It becomes necessary to obtain fairly accurate estimates of the payload capabilities of advanced propulsion vehicles for various interplanetary missions. In Ref. 1, there appeared the results from a series of trajectories to the planets Venus and Mars. An optimum variable thrust program was used to generate these trajectories. Moreover, certain terminal conditions, such as the orientation of the terminal orbit and the terminal position on the orbit, were left unspecified, and corresponding transversality conditions derived from the calculus of variations were satisfied instead.

This paper is concerned with the problem in which all end conditions, as determined by the planetary ephemerides, are specified, and the main purpose is to show the manner in which the propulsion requirements vary both with flight time and with launch date. This procedure is analogous to the problem in ballistic trajectories in which the velocity increments required for interplanetary missions are determined (2,3).[3] In advanced propulsion trajectories, however, the propulsion intervals constitute a significant portion of the trajectory, and, therefore, the thrust program employed becomes quite important in payload studies, and optimization theory as applied to the trajectory analysis is of considerable use. A comparison of vehicle performance will be made between the use of an optimum variable thrust program and the use of an optimum constant thrust program.

Optimum Thrust Equations

In order to develop an optimum thrust program that extremizes some terminal quantity indicative of vehicle performance, it is necessary to include the constraints of the system. For the power-limited propulsion system, the constraints are the equations of motion of the vehicle and an equation describing the fact that the amount of kinetic power contained in the exhaust propellant is constrained. Generally, the kinetic power depends on the efficiency of power conversion from the nuclear powerplant of the vehicle, and the efficiency, in turn, is dependent on the exhaust velocity employed. In this treatment, the kinetic power is constant, which is the case for the constant thrust program since the exhaust velocity is constant. The variable thrust program possesses a variable exhaust velocity, and thus performance figures obtained from this program are optimistic for two reasons: 1) the thrust program is unconstrained; and 2) the variation of efficiency is neglected. On the other hand, performance figures from the constant thrust program tend to be conservative but are more realistic.

The constraining equations of motion are

$$\ddot{\mathbf{r}} + \nabla V - \mathbf{a} = \mathbf{0} \qquad [1]$$

and the power-limited constraint is

$$\dot{\mu} + (\beta/c^2)\alpha_p = 0 \qquad [2]$$

where $\mathbf{r}$ is the position vector of the vehicle, V the potential of the force field, and $\mathbf{a}$ the thrust acceleration with the magnitude

$$a = -\dot{\mu}\, c/\mu = (\beta/\mu c)\alpha_p \qquad [3]$$

The quantity μ is the normalized mass of the vehicle [$\mu(t_0) = 1$]; β is twice the kinetic power in the rocket exhaust per unit initial mass of the vehicle and is, therefore, a constant dependent on the specific mass and size of the powerplant. The quantity c is the exhaust velocity, and α_p is a switching parameter with the value 1 during propulsion periods and 0 during coasting periods.

A Mayer formulation (4) of the calculus of variations has been applied to both the constant and variable thrust cases to obtain the optimum thrust equations. The optimum thrust equations have been derived in Ref. 5 and are summarized here. The thrust program is determined by

$$\ddot{\boldsymbol{\lambda}} + (\boldsymbol{\lambda}\cdot\nabla)\nabla V = \mathbf{0} \qquad [4]$$

$$\mathbf{a} = \begin{cases} \text{constant } \boldsymbol{\lambda} & \text{(variable thrust)} \\ \dfrac{\text{constant}}{\mu}\dfrac{\boldsymbol{\lambda}}{\lambda}\alpha_p & \text{(constant thrust)} \end{cases} \qquad [5]$$

where $\boldsymbol{\lambda}$ is the Lagrange multiplier vector, and the constant in Eq. [5] is determined from boundary conditions. It may be shown that no coasting periods occur in the variable thrust program (5–7). In the constant thrust program the switching function $L(t)$ generated by the equation

$$\dot{L} = \dot{\lambda}/\mu \qquad [6]$$

determines the periods of propulsion and coast by the conditions

$$\begin{array}{ll} L > 0 & \alpha_p = 1 \\ L < 0 & \alpha_p = 0 \end{array} \qquad [7]$$

In the case where V is explicitly independent of time, it may be shown that the equations of motion (Eq. [1]) and the Euler equations (Eq. [4]) possess a first integral in the form

Received by ARS January 31, 1962; revised June 13, 1962.

[1] Research Group Supervisor. Member ARS.

[2] Research Specialist. Member ARS.

[3] Numbers in parentheses indicate References at end of paper.

$$\begin{aligned} \dot{\lambda}\cdot\dot{r} + \lambda\cdot\nabla V - \tfrac{1}{2}a\lambda &= K_2 \quad \text{(variable thrust)} \\ \dot{\lambda}\cdot\dot{r} + \lambda\cdot\nabla V - a\mu L &= K_2 \quad \text{(constant thrust)} \end{aligned} \qquad [8]$$

Propulsion System Optimization

By eliminating c from Eqs. [2] and [3] and integrating, one obtains

$$\frac{1}{\mu_1} = \frac{1}{\mu_0} + \int_{t_0}^{t_1} \frac{a^2}{\beta}\, dt \qquad [9]$$

which is the so-called rocket equation for power-limited propulsion systems. The quantity

$$J = \int_{t_0}^{t_1} a^2\, dt \qquad [10]$$

appearing in Eq. [9] is analogous to the concept of characteristic velocity in chemical rocket trajectories and is a convenient index of rocket performance. Since in this treatment β remains constant, any thrust program maximizing μ_1 also minimizes J. In the variable thrust program, the exhaust velocity is determined through Eqs. [2, 3, and 5]. In the constant thrust program, for a particular mission, any exhaust velocity below some maximum value yields an optimum trajectory. These trajectories possess different lengths of coasting and different values of J. There exists, in general, an optimum exhaust velocity yielding a minimum J. It is shown in Ref. 5 that the condition

$$\int_{t_0}^{t_1} \alpha_p \left(2L - \frac{\lambda}{\mu}\right) dt = 0 \qquad [11]$$

guarantees an extremal in J with respect to the exhaust velocity for the constant thrust program.

Missions and Terminal Conditions

The position and velocity coordinates must satisfy specified values or functions at both end points of the rendezvous trajectory. In planetary-rendezvous missions, six terminal quantities must be specified at each end point. In Ref. 1, it was described how these quantities were grouped into five orbital quantities that determine the shape and orientation of the terminal ellipse and are essentially time-invariant, and one time-varying quantity indicating the rendezvous position on the terminal ellipse. The reader is referred to Ref. 1 for a description of these quantities.

It was also shown in Refs. 1, 5, and 8 (see Appendix) that for each terminal condition left unspecified there results a corresponding transversality condition to be satisfied at the end point instead. Satisfying these transversality conditions yields extremals in the quantity being optimized with respect to the unspecified terminal conditions. In particular, it was shown that if the rendezvous position (say, true anomaly) on the terminal ellipse is left unspecified at either end point, the transversality condition

$$\dot{\lambda}\cdot\dot{r} + \lambda\cdot\nabla V = 0 \qquad [12]$$

should be satisfied at the corresponding end point(s). If, in addition, the transfer angle between the initial and final point of the trajectory is unspecified, then the z component of the constant vector $\bar{K}_1$, given by

$$\bar{K}_1 = r \times \dot{\lambda} - \dot{r} \times \lambda \qquad [13]$$

must be zero (1,5,8). The z direction is perpendicular to the plane containing the transfer angle (the angle θ as defined in Ref. 1). Eq. [13] holds in any central force field, and the z component of $\bar{K}_1$ is the same constant K_1 appearing in Ref. 1 in the spherical coordinate formulation of the Euler-Lagrange equations. These two transversality conditions will be used to interpret the behavior of the performance

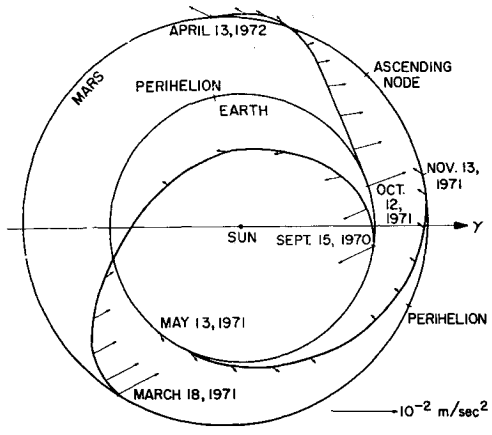

Fig. 1 Mars rendezvous trajectories, 184 days flight time, variable thrust program, ecliptic projection

requirements with launch date. One further transversality condition will be used in the sequel. Suppose the initial and final conditions are determined by ephemerides and are, therefore, functions of only the launch and arrival dates, respectively. It is shown in Ref. 8 that, if the launch date t_0 is unspecified for a fixed flight time, satisfying the transversality condition

$$[\dot{\lambda}\cdot\dot{r} + \lambda\cdot\nabla V]_{t_0}^{t_1} = 0 \qquad [14]$$

yields an extremal in the quantity being optimized with respect to launch date.

Interplanetary Trajectories

The optimum thrust equations, the constraining equations, and various ancillary equations have been programmed in three dimensions for numerical solution on an IBM 7090. Eq. [8] is used to check the accuracy of the numerical integrations. A Newton-Raphson (9) search method has been used to obtain converged trajectories with specified boundary conditions. By the use of this method in conjunction with certain prediction schemes (9), it has been possible to generate wholesale amounts of trajectories with only a moderate consumption of machine time. By this technique, the indirect method of the calculus of variation has been eminently successful when applied to interplanetary trajectories, even in three dimensions where six and sometimes seven quantities are specified at the final point.

The results from a series of three-dimensional rendezvous trajectories from Earth to Mars are presented. These trajectories use the actual positions and velocities of these planets during the era 1968 to 1971 as initial and final conditions. Only the gravitational field of the sun was included in these calculations. As an example of the nature of these trajectories, Fig. 1 shows three trajectories of the same flight time launched at different dates during the synodic era 1970 to 1971. The variable thrust program was used to generate these trajectories, and the arrows on the trajectories indicate the direction and magnitude of the thrust acceleration. This figure is an ecliptic projection; the effect of the third dimension is small and has been discussed in Ref. 1. Fig. 2 shows the same trajectories generated by the constant thrust program, and the similarities should be noted. These trajectories possess an optimum coast period in the sense that Eq. [11] is satisfied for a fixed value of β of 100.0 m^2/sec^3; the periods of coast have been indicated. The September 15, 1970 and October 12, 1971 trajectories are probably not feasible missions; the thrust acceleration vector at the final point of these two trajectories in Fig. 2 has increased to more than twice the size of the initial value, indicating that less than half the vehicle mass remains. The maximum mass loss that can be sustained by an advanced propulsion vehicle if

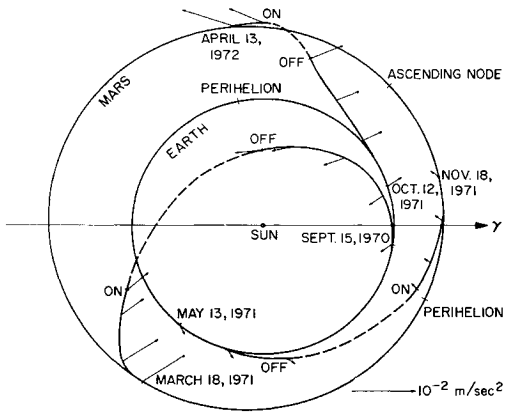

Fig. 2 Mars rendezvous trajectories, 184 days flight time, constant thrust program with optimum coast, ecliptic projection

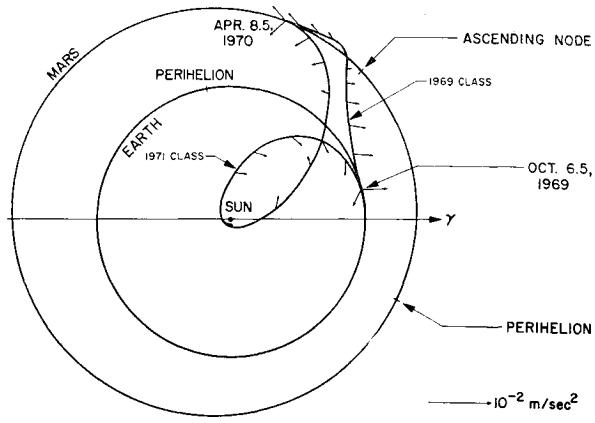

Fig. 4 Mars optimum rendezvous trajectories with equal $\int_{t_0}^{t_1} a^2 dt$, flight time, and launch date, 184 days flight time, variable thrust program

it is to deliver a significant payload is about half the initial mass.

A series of trajectories with different launch dates and flight times has been obtained. Fig. 3 shows the variation of J with heliocentric launch date for many flight times using the variable thrust program. With this figure, it is possible to determine the "launch period" that is available for given maximum value of J and a specified range of flight times. At the launch date where minimum J occurs for a given flight time, the transversality condition in Eq. [14] is satisfied. The May 13, 1971 trajectory shown in Figs. 1 and 2 has nearly the optimum launch date for a 184-day flight time and for this synodic era.

The curves in Fig. 3 are not unique because there exist classes of trajectories yielding extremals in J which, for a given launch date and flight time, rendezvous with Mars after executing an arbitrary number of circuits around the sun in either the forward or retrograde direction. Of particular interest are those classes of trajectories which make one less and one more circuit around the sun and which correspond to the optimum sets in the neighboring synodic eras. As an example, the class of trajectories which is optimum in the 1971 synodic era is generally characterized by an additional circuit around the sun when flown in the 1969 era. For a given flight time there clearly exists a launch date that is a trade-off point and for which, for earlier dates, the optimum path is obtained by subtracting 2π from the transit angle required to rendezvous Mars. Fig. 4 shows an example from each of these two classes of trajectories using a variable thrust program. Both of these trajectories have the same

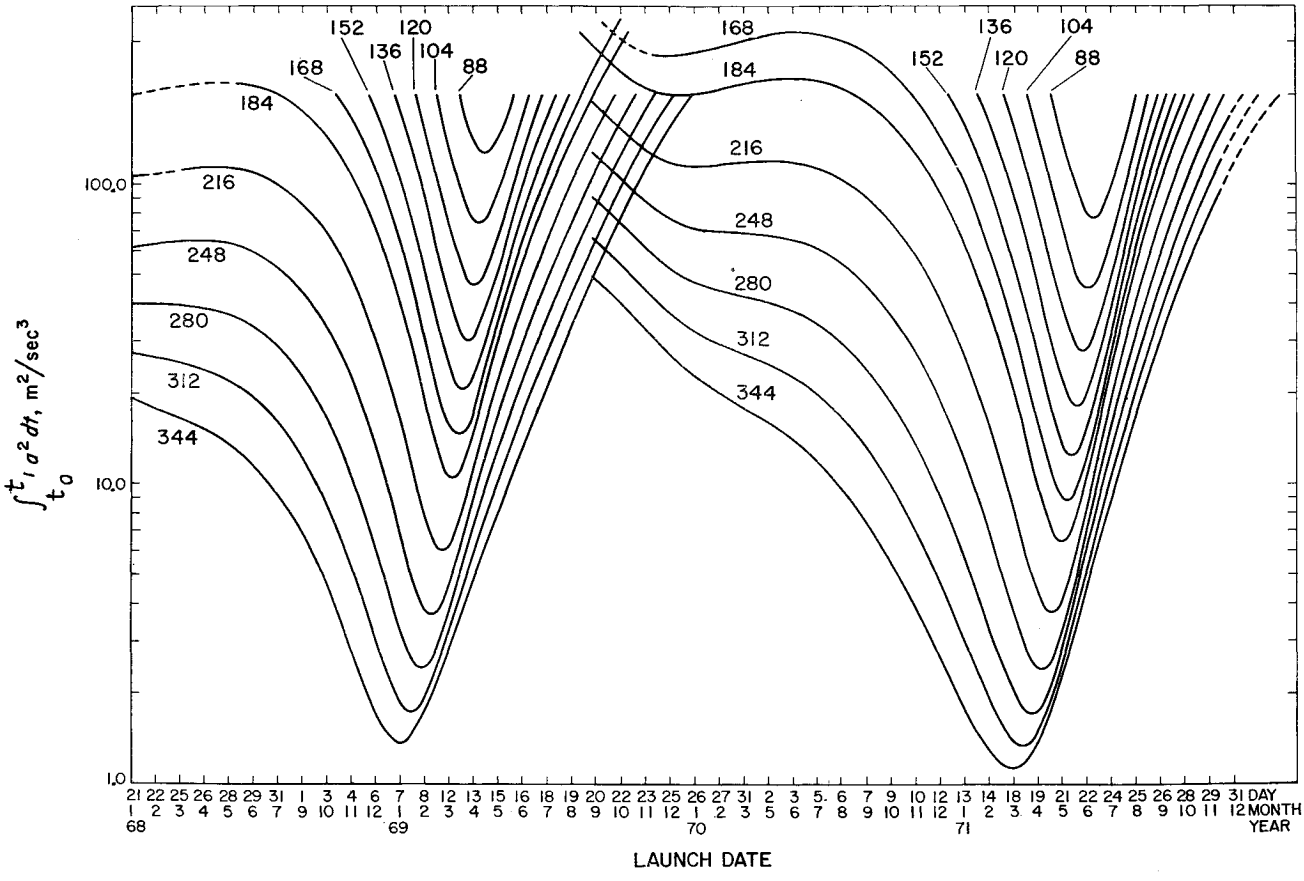

Fig. 3 Earth-Mars rendezvous trajectories, variable thrust program, $\int_{t_0}^{t_1} a^2 dt$ vs launch date for constant flight time (days), 1968 to 1972

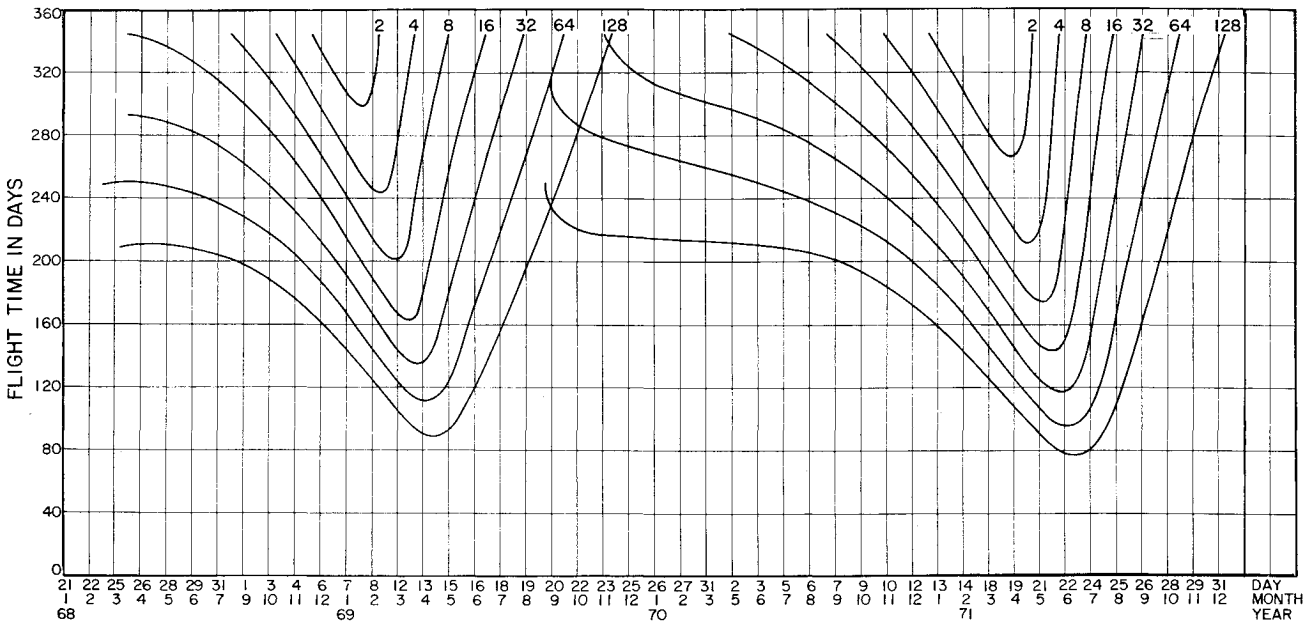

Fig. 5 Earth-Mars rendezvous trajectories, variable thrust program, flight time vs launch date for constant $\int_{t_0}^{t_1} a^2 dt$ (m²/sec³)

launch date and flight time and possess the same value of J but use radically different thrust programs in carrying out the mission. The two classes of trajectories which are optimum for the 1969 and 1971 synodic eras are shown on Fig. 3, and the trade-off points in launch date are clearly seen. The trajectories of the left-hand wing of the 1971 class appearing in 1969 to 1970 are probably only of academic interest, since the values of J for these curves are so high. For the presently estimated state of the art of advanced propulsion technology, missions with values of J greater than around 50 m³/sec² are probably not feasible. The local extremals in J with launch date which appear in the wings also fulfill the condition in Eq. [14].

The increased steepness on the ascending branches of these curves may be explained in terms of the decreasing transit angle of the trajectory with increasing launch date as shown

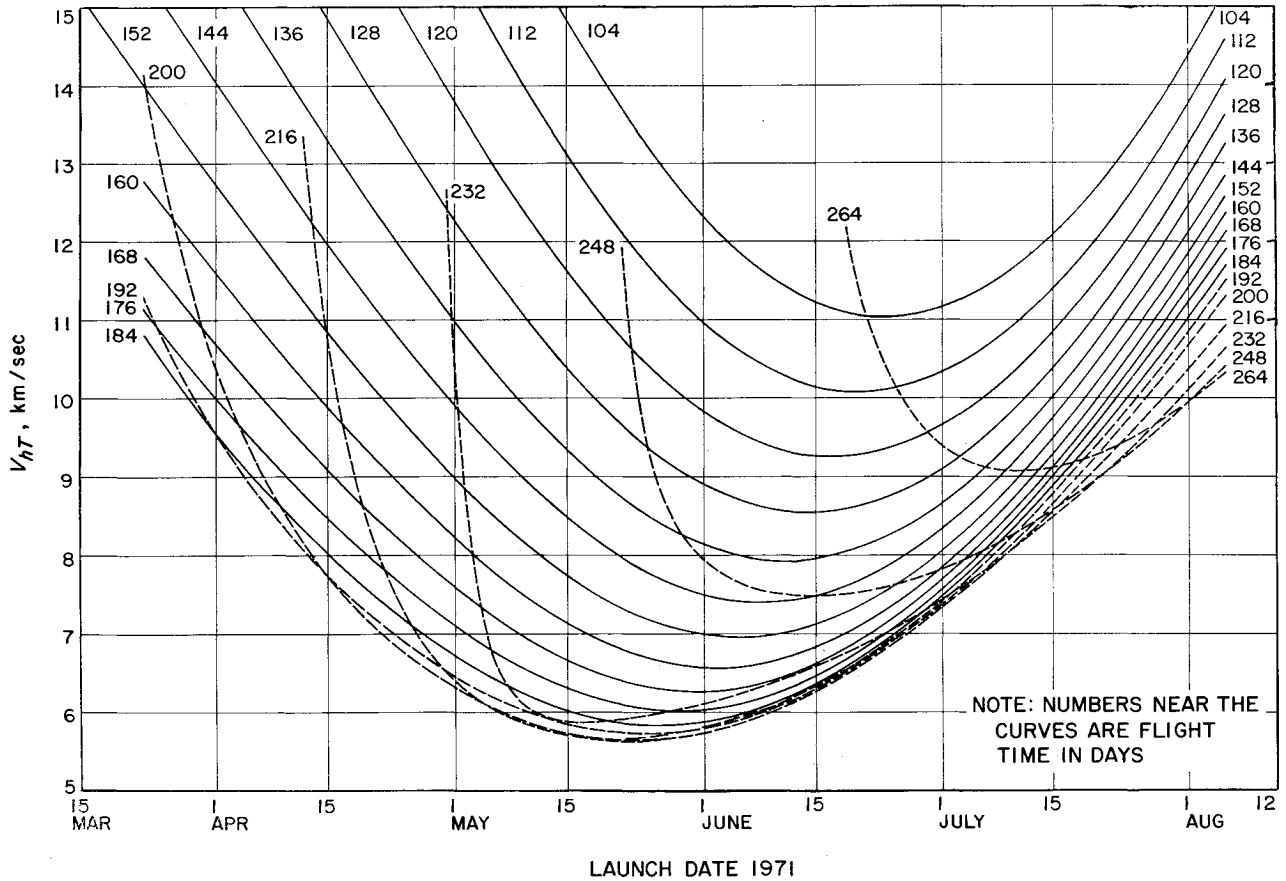

Fig. 6 Type I Mars 1971 ballistic trajectories, sum of geocentric and areocentric hyperbolic excess speeds vs launch date for constant flight time

Table 1 Three-dimensional trajectories, 184-day flight

Launch date (1971)	Constant thrust $\int a^2 dt$ $\beta = \infty$	Constant thrust $\int a^2 dt$ $\beta = 100.0$	Constant thrust μ_1 $\beta = 100.0$	Variable thrust $\int a^2 dt$
Feb. 14	45.477	43.131	0.699	37.373
March 2	33.980	32.406	0.755	27.733
March 18	24.608	23.640	0.809	19.931
April 3	17.298	16.757	0.856	13.938
April 19	11.949	11.678	0.895	9.703
May 5	8.516	8.404	0.922	7.187
May 13	7.596	7.546	0.930	6.576
May 21	7.340	7.351	0.932	6.406
June 6	8.966	9.110	0.917	7.459
June 22	13.180	13.565	0.881	10.558
July 8	20.150	21.070	0.826	16.046
July 24	30.417	32.479	0.755	24.395
Aug. 9	44.691	49.038	0.671	36.217
Aug. 17	53.583	59.766	0.626	43.648

Table 2 Two-dimensional trajectories, 184-day flight

Launch date (1971)	Constant thrust $\int a^2 dt$ $\beta = \infty$	Constant thrust $\int a^2 dt$ $\beta = 100.0$	Constant thrust μ_1 $\beta = 100.0$	Variable thrust $\int a^2 dt$
Feb. 14	45.165	42.864	0.700	37.230
March 2	33.714	32.171	0.757	27.597
March 18	24.379	23.431	0.810	19.796
April 3	17.096	16.567	0.858	13.798
April 19	11.762	11.498	0.897	9.555
May 5	8.334	8.225	0.924	7.032
May 13	7.414	7.364	0.931	6.418
May 21	7.161	7.171	0.933	6.247
June 6	8.801	8.942	0.918	7.303
June 22	13.023	13.401	0.882	10.413
July 8	20.003	20.914	0.827	15.918
July 24	30.289	32.339	0.756	24.292
Aug. 9	44.588	48.920	0.672	36.139
Aug. 17	53.492	59.659	0.626	43.584

in Figs. 1 and 2. For launch dates past the optimum point, the percentage change in transit angle is greater than for equally distant launch dates preceding the optimum point. As the positions of Earth at launch and Mars at arrival approach opposition, a thrust program more radical (as indicated in the October 12, 1971 trajectory) than the program for optimal transfer is required. This same effect occurs in ballistic trajectories.

The year 1971 is a "vintage year" for advanced propulsion trajectories (and also for ballistic trajectories) in the sense that the minima of these curves possess smaller values for this year than they do for immediately preceding or succeeding synodic eras. Notice in Fig. 3 that the minima in 1969 lie at a value of J higher than do the corresponding minima in 1971. This phenomenon can be interpreted in terms of the fact that, for 1971, the transversality condition in Eq. [12] is nearly satisfied for all flight times at both the initial and final points of the trajectory at the optimum launch dates. Searching for the optimum synodic era is tantamount to removing the coupling supplied by the ephemerides between planetary positions and launch and arrival dates. In this case, the positions on the initial and final ellipses become unspecified and Eq. [14] decomposes into Eq. [12], which must be satisfied at both terminal points (see Appendix). In 1971, the Earth-Mars distance at opposition is smaller than in neighboring synodic eras; this phenomenon repeats approximately every 15 years or every seven synodic periods. It is known, however, that the optimum point of rendezvous at Mars is not at perihelion but rather at some point past perihelion where the radial velocity is, in general, outward (10).

Fig. 5 exhibits contours of equal J with flight time vs heliocentric launch date. The minima of these curves correspond to minimum time trajectories for a given value of J, and the transversality condition in Eq. [15] is also satisfied at this point. The locus of minimum flight for a given J will pass, for zero flight time, near the date of Earth-Mars opposition.

In order to isolate the range of variation of minimum J with synodic era, a series of trajectories was run in which the transversality condition in Eq. [12] was satisfied at both terminal points. Since the orbit of Earth is nearly circular, this approximation was made in these computations. In this case, it can be shown (see Appendix) that Eq. [12] implies that the z component of $\bar{K}_1$ is zero, simplifying the analysis somewhat. Fig. 14 of Ref. 1 shows the variation in J with flight time for Mars rendezvous trajectories in which Eq. [12] is satisfied at the final point of the trajectory and the constant K_{1_z} is zero. Both local minima and local maxima occur when these conditions are satisfied. The lower curve of this figure corresponds to rendezvous at the optimum orbital point, and the upper curve corresponds to rendezvous at the least optimum point, which is generally approximately 180° away from the optimum point. The optimum rendezvous points are functions of flight time (1,10). These two curves bound the range of variation of minimum J with synodic period using a variable thrust program. It should be observed that the minima of the 1971 curves lie almost exactly along the lower curve. At three or four synodic periods before or after 1971, the Earth-Mars configuration at optimum launch date is such that trajectories rendezvous near the least optimum point, and the minima therefore lie near the upper curve.

The estimates of propellant requirement for heliocentric transfer as given in Fig. 3 tend to be slightly conservative because of the neglect of the masses of the departure and arrival planets. In spiralling away from Earth, for example, the geocentric velocity at escape is, typically, around 1 km/sec. It may be shown (10) that the velocity at escape is proportional to the fourth root of the thrust acceleration and the gravitational constant of the central planet, and so the velocity at escape changes little with the thrust acceleration employed. In any case, this velocity, although small compared to the 30-km/sec orbital velocity of Earth, can be used, if properly directed, to obtain a reduction in the J required for the heliocentric portion of the flight. Preliminary studies suggest that approximately 15% reduction in J for the heliocentric flight can be obtained by taking into account the masses of the departure and arrival planets.

Finally, it is interesting to compare the propulsion requirements for an advanced propulsion vehicle with those for a ballistic vehicle. Fig. 6 shows the sum of the geocentric and Mars-centered hyperbolic-excess speeds vs launch date for various flight times. This figure is obtained from results appearing in Ref. 3, in which heliocentric conics were fitted through Earth and Mars as explained in Refs. 2 and 3. The similarities between Figs. 3 and 6 should be noted. For a given flight time, the optimum launch dates are about the same for these two types of trajectories; however, the "firing period" for the advanced propulsion vehicle is somewhat wider than that for the ballistic vehicle.

Comparison of Variable and Constant Thrust Programs

The degradation in vehicle performance resulting from using a less optimum thrust program is of interest. In Ref. 5 a comparison was made between the variable thrust program and the constant thrust program with both an optimum coast period and no coast. It was shown (consult Fig. 7 of Ref. 5) that for optimum launch dates the increase in J in the constant thrust program with optimum coast is about 15%

over the variable thrust program and about 30% in the case of no coast. A 15% increase in J corresponds, typically, to about a 3% decrease in μ, as may be verified from Eq. [9]; that is, for small variations

$$\delta\mu_1 = -\mu_1(1 - u_1)\delta J/J \qquad [15]$$

For trajectories launched at dates other than the optimum launch date, the percentage difference in J between the two thrust programs varies somewhat. Tables 1 and 2 illustrate the difference between these two programs for various launch dates for a 184-day flight. The transversality condition in Eq. [11] is satisfied in the constant thrust program using values for β of 100 m^2/sec^3 and infinity (constant thrust acceleration). In addition, the results from a corresponding set of two-dimensional trajectories are presented to show the difference between two- and three-dimensional analysis for interplanetary trajectories. The differences are small, as already pointed out in Ref. 1. The largest relative effect occurs near the optimal launch date, which reflects the fact that the additional propulsion requirement for the out-of-ecliptic dimension is relatively insensitive to the launch date.

The variable thrust program has been used in the majority of the numerical computations for several reasons. The performance results constitute a unique upper bound independent of the propulsion system design; the computation time is generally less than with the constant thrust program because 1) the dimension of the iteration matrix is smaller since no propulsion system optimization is required, and 2) the variable thrust equations seem somewhat more stable, computationally, and converge more rapidly. The use of a constant thrust acceleration program (infinite β) with optimum coast also has the advantages of being independent of the propulsion system design and yields more conservative performance results. Experience has shown that this program is nearly as stable and economical as the variable thrust program and requires only one additional dimension in the iteration matrix: namely, the fulfillment of Eq. [11] at the final point of the trajectory. The present policy in parametric mission feasibility studies is to employ both of these programs to obtain performance figures that bracket the performance capabilities of an actual advanced propulsion vehicle.

Appendix: Terminal Conditions and Optimum Launch Dates

If certain terminal quantities are undetermined by the boundary conditions and the condition for an extremal in J, there results from the calculus of variations (4,5,8) a corresponding transversality expression for each undetermined terminal quantity. Satisfying a transversality expression yields an extremal in J with respect to the corresponding undetermined terminal quantity and, in addition, the optimal value for this quantity.

Consider the case in which the kinematic state variables are specified at both ends of the trajectory by explicit functions of time which, in the case of planetary rendezvous, are simply the ephemerides of the departure and arrival planets. The positions and velocities $\bar{r}$, $\bar{v}$ at the terminal points may be expressed in the form

$$\left.\begin{matrix} \mathbf{r}(t_0) - \mathbf{r}^{(0)}(t_0) = 0 & \mathbf{r}(t_1) - \mathbf{r}^{(1)}(t_1) = 0 \\ \mathbf{v}(t_0) - \mathbf{v}^{(0)}(t_0) = 0 & \mathbf{v}(t_1) - \mathbf{v}^{(1)}(t_1) = 0 \end{matrix}\right\} \qquad [A1]$$

The superscripts 0 and 1 denote the functions corresponding to the ephemerides of the departure and arrival planets, respectively. Furthermore, suppose that the flight time $t_1 - t_0$ is held fixed but that the launch date t_0 is not specified. For three dimensions, 14 boundary conditions have been specified. (These are Eq. [A1], fixed flight time, and initial mass of unity.) The launch date is unspecified, and, consequently, there is one transversality condition available which holds at the optimum launch date extremizing J. Upon applying the calculus of variations (8), one obtains for this expression

$$(\boldsymbol{\lambda}\cdot\dot{\mathbf{v}}^{(1)} - \dot{\boldsymbol{\lambda}}\cdot\mathbf{v})\,|_{t_1} - (\boldsymbol{\lambda}\cdot\dot{\mathbf{v}}^{(0)} - \dot{\boldsymbol{\lambda}}\cdot\mathbf{v})\,|_{t_0} = 0 \qquad [A2]$$

Since the planets travel in the same potential field as the vehicle, it follows that the condition

$$[\dot{\boldsymbol{\lambda}}\cdot\dot{\mathbf{r}} + \boldsymbol{\lambda}\cdot\nabla V]\,|_{t_1}^{t_0} = 0 \qquad [A3]$$

is the transversality condition for optimum launch date. For the variable thrust program, it is easily seen from Eq. [8] that this condition is satisfied when the thrust acceleration is equal at the initial and final points of the trajectory.

In Ref. 1 a spherical coordinate system has been employed, and the kinematic boundary conditions have been expressed in terms of the orbital elements E, h, i, ω, Ω, and Ψ (see Fig. 2 and Eqs. [17–22] of Ref. 1). It was stated that, if the position on the terminal orbit Ψ is left unspecified but with fixed flight time (and no dependence on launch date), the transversality condition that should be satisfied for optimum rendezvous point (and least optimum, also) was given by

$$M + N + K_1 h_\Phi / r^2 \cos\Phi = 0 \qquad [A4]$$

where these symbols are defined in Ref. 1. Using Eq. [17] of Ref. 1 and Eq. [8] of this text, it follows that this condition is equivalent to

$$(\dot{\boldsymbol{\lambda}}\cdot\dot{\mathbf{r}} + \boldsymbol{\lambda}\cdot\nabla V)\,|_{t_\nu} = 0 \qquad \nu = 0, 1 \qquad [A5]$$

Using orbital elements and including a launch date dependency, only the quantity Ψ is a function of the launch and arrival dates through the ephemerides, and it may be expressed in the form

$$\Psi(t_0) - \Psi^{(0)}(t_0) = 0 \qquad \Psi(t_1) - \Psi^{(1)}(t_1) = 0 \qquad [A6]$$

It is clear that Eq. [A3] must still hold for optimum launch date. However, if one passes through synodic eras seeking the optimum synodic era, this is tantamount to removing the coupling between orbital positions and launch and arrival dates in Eq. [A6]; the terminal values of Ψ are, in effect, unspecified, and it follows that Eq. [A3] decomposes into the two conditions in Eq. [A5], which holds in the optimum synodic era at the optimum launch date in that synodic era. In actuality, Eq. [A5] is never exactly satisfied at both the initial and final point, but in the year 1971 these conditions will be nearly met.

If either the initial or the final orbit is circular and the launch date dependency is removed, it is unnecessary to specify the transit angle $\theta(t_1) - \theta(t_0)$. In the spherical coordinate formulation of Ref. 1, it was shown that a constant K_1 results from the cyclic nature of the variable θ. If θ does not explicitly appear in the boundary conditions nor in the expression to be extremized, it is easily shown (8) that K_1 is zero. Consequently, if the terminal orbital position and the transit angle (or alternately, the longitude of the line of nodes Ω) are unspecified, it follows from Eq. [A4] that both Eq. [A5] and a zero value for K_1 are implied.

It should be obvious that there are any number of transversality conditions for this problem which may be developed for each unspecified variable. As a final example, consider the problem of finding the optimum launch date for any flight time when the transit angle is held fixed. One may draw curves of constant transit angle on Fig. 5. These curves depart slightly from straight lines because of the planetary eccentricities but are sloped upward and to the right, that is, increasing flight time with increasing launch date. As one travels along one of these curves, there is an optimum launch date and flight time corresponding to a minimum J. Using the sole constraint that $\theta(t_1) - \theta(t_0)$ is a constant, it may be verified that the condition

$$[(K_2 + \dot{\boldsymbol{\lambda}}\cdot\dot{\mathbf{r}} + \boldsymbol{\lambda}\cdot\nabla V)\dot{\theta}^{-1}]_{t_0}^{t_1} = 0 \qquad [A7]$$

yields the optimum launch date.

Acknowledgment

The authors wish to express their sincere gratitude to D. E. Richardson, of the Jet Propulsion Laboratory, who collaborated in the development of the computer program and to Helen Ling for her assistance in the numerical results.

References

1 Melbourne, W. G., "Three-dimensional optimum thrust trajectories for power-limited propulsion systems," ARS J. **31**, 1723–1728 (1961).
2 Breakwell, J. V., Gillespie, R. W., and Ross, S., "Researches in interplanetary transfer," ARS J. **31**, 201–208 (1961).
3 Clarke, V. C., Bollman, W. E., and Scholey, W. J., "Design parameters for ballistic interplanetary trajectories, Part I: One-way transfer to Mars and Venus," Jet Propulsion Lab., Pasadena, Calif., TR 32-77 (March 1, 1962).
4 Bliss, G. A., *Lectures on the Calculus Variations* (University of Chicago Press, Chicago, 1946), Chaps. 1 and 7.
5 Melbourne, W. G. and Sauer, C. G., Jr., "Optimum thrust programs for power-limited propulsion systems," Jet Propulsion Lab., Pasadena, Calif., TR 32-118 (1961); also Astronaut. Acta (to be published).
6 Irving, J. H., *Space Technology*, edited by H. S. Seifert (John Wiley and Sons Inc., New York, 1959), Chap. 10.
7 Leitmann, G., "Minimum transfer time for a power-limited rocket," J. Appl. Mech. **28**, 171–178 (1961).
8 Melbourne, W. G. and Sauer, C. G., Jr., "Optimum interplanetary rendezvous trajectories for power-limited vehicles," Jet Propulsion Lab., Pasadena, Calif., TR 32-226 (1962).
9 Melbourne, W. G., Richardson, D. E., and Sauer, C. G., "Interplanetary trajectory optimization with power-limited vehicles," Jet Propulsion Lab., Pasadena, Calif., TR 32-173 (1961).
10 Melbourne, W. G., "Interplanetary trajectories and payload capabilities of advanced propulsion vehicles," Jet Propulsion Lab., Pasadena, Calif., TR 32-68 (1961).

JANUARY 1963 AIAA JOURNAL VOL. 1, NO. 1

Effect of Finite Thrusting Time in Orbital Maneuvers

CHONG-HUNG ZEE[1]

Curtiss-Wright Corporation, Wood-Ridge, N. J.

The effect of finite thrusting time in orbital maneuvers is investigated for Hohmann-type transfers. A closed form solution of the trajectory during thrusting is obtained by assuming that a constant thrust is applied normal to the focal radius and that the change of the radial position of the rocket is small. A numerical example is presented to show the thrusting time, thrust level, propellant consumption, and the conic trajectories following the powered flight paths, etc., in comparison with the ordinary impulsive thrust case. Finally, calculations of the lead angle and the lead time are introduced based on the analysis presented in this paper.

Nomenclature

A = $\dot{m}\bar{c}/M_0 g_0$, dimensionless
B = $(\dot{m}/M_0)\,(r_0/g_0)^{1/2}$, dimensionless
C = $V_e/(g_0 r_0)^{1/2}$, dimensionless
$\bar{c}$ = effective average exhaust velocity of the jet, fps
D = $V_r/(g_0 r_0)^{1/2}$, dimensionless
E = energy per unit mass of rocket, ft-lb/slug
e = eccentricity of the elliptical transfer orbit, dimensionless or base of natural logarithms
F = $\dot{m}\bar{c}$ = total thrust, lb
g_0 = acceleration due to gravity at distance r_0 from the center of attraction, ft/sec^2
g_e = acceleration due to gravity at earth surface, say, 32.2 fps
l = semilatus rectum of the transfer elliptical orbit, ft
$\dot{m}$ = constant flow rate of propellant mass, slug/sec
M_0 = mass of rocket at the beginning of thrusting, slug
M_p = propellant mass consumed, slug
ΔM_p = additional propellant mass consumed due to finite thrusting time, slug
n = number denoting initial acceleration or thrust level, dimensionless
r = distance from the center of attraction to the rocket at any time during thrusting, ft
r_1 = radius of final circular orbit, ft
r_f = distance from the center of attraction to the rocket at the end of thrusting, ft
r_0 = distance from the center of attraction to the rocket at the beginning of thrusting, ft
t = time measured from the beginning of thrusting, sec
t_f = finite thrusting time, sec
t_l = lead time (time required to travel the lead angle), sec
V_c = $(g_0 r_0)^{1/2}$ = circumferential velocity of a circular orbit with radius r_0, fps
V_f = velocity of the rocket after the impulsive thrust or at the end of thrusting, fps
V_r = $(dr/dt)_0$ = radial velocity of the rocket at the beginning of thrusting, fps
V_θ = $r_0(d\theta/dt)_0$ = transverse velocity of the rocket at the beginning of thrusting, fps
θ = polar angle, measured from the initial line coincided with the radius vector r_0, rad
θ_f = angular displacement of the rocket at the end of thrusting, rad
ψ = lead angle, angle between the radius vector r_0 and the apsides line of transfer orbit, rad
ρ = r/r_0, dimensionless
ρ_f = r_f/r_0, dimensionless
τ = $(g_0/r_0)^{1/2}t$, dimensionless
μ = gravitational constant, ft^3/sec^2
$(\,)_0$ = denotes the quantity in the parentheses at $t = 0$

Subscript

I = impulsive thrust case

IT is generally assumed that the thrusting time is zero for all impulsive thrusts in orbital maneuvers. However, for practical reasons, this case does not exist, and nonzero thrusting times must be considered. Transfer orbits then consist of powered flight paths, which are the trajectories of a rocket during the finite thrusting time intervals, and nonpowered flight or conic paths.

If, at a certain point in an orbit, a constant thrust is applied to a rocket, different thrust levels will result in different powered flight paths, even though the total propellant consumption (or the total impulse that is the product of the thrust and the thrusting time) remains the same. The conic paths following the powered flight paths will also change

Received by ARS February 28, 1962; revised July 19, 1962.
[1] Project Engineer, Engineering Department, Wright Aeronautical Division.